

Recent Developments in High-Harmonic Fast Wave Physics in NSTX*

B.P. LeBlanc¹, R.E. Bell¹, P. Bonoli², R. Harvey³, W.W. Heidbrink⁴, J.C. Hosea¹, S.M. Kaye¹, D. Liu⁵, R. Maingi⁶, M. Ono¹, M. Podestà¹, C.K. Phillips¹, P.M. Ryan⁶, A.L. Roquemore¹, G. Taylor¹, J.R. Wilson¹ and the NSTX Team

¹PPPL, Princeton, NJ 08543, USA, ²PSFC,-MIT, Cambridge, MA,02139,

³CompX, Del Mar, CA 92014, USA, ⁴Department of Physics and Astronomy, UCI, CA 92617, USA, ⁵University of Wisconsin, ⁶ORNL, Oak Ridge, TN 37831, USA

Understanding the interaction between ion cyclotron range of frequency (ICRF) fast waves and the fast-ions created by neutral beam injection (NBI) is critical for future deuterium-tritium plasma devices such as ITER, which rely on a combination ICRF and NBI heating to reach a regime dominated by alpha-particle heating. Experiments in NSTX which use High-Harmonic Fast-Wave (HHFW) ICRF¹ and NBI heating show a strong competition between electron heating via Landau damping and transit-time magnetic pumping, and rf acceleration of NBI generated fast ions. The HHFWs exhibit rapid single pass absorption in high beta (10-40%) NSTX discharges so that rf coupling efficiency is dominated by edge losses originating near the antenna. Understanding and mitigating some of the rf power loss mechanisms outside the last closed flux surface (LCFS) has resulted in improved rf heating inside the LCFS. First wall lithium coating was found an effective tool in achieving these goals. A similar magnitude of rf power is absorbed by the fast ions and electrons within the LCFS.

An array of twelve vertical current elements driven by six 30-MHz transmitters form a flexible antenna system² able to launch toroidally balanced or directed wave spectra characterized by absolute values of k_{\parallel} spanning 3 to 13 m^{-1} . Coupled power typically ranges from 1 to 4 MW, with up to 6 MW available. Mechanisms that reduce rf power reaching the plasma inside the LCFS include parametric decay instability (PDI) ion heating³, which can absorb up to 20% of the power, and excitation of surface waves⁴ which disperse wave power outside the LCFS. Recent improvements in heating efficiency at lower k_{\parallel} , important for current drive (e.g. $k_{\parallel}=-8\text{m}^{-1}$), have been ascribed to a reduction of the latter loss mechanism and partially attributed to lithium wall coating⁵. Lithium coatings lower the density at the antenna, thereby moving the critical density for perpendicular fast-wave propagation away from the antenna hence reducing the rf power that flows to the vessel wall and interior components. Visible and infrared camera images during rf-heated NBI induced H-mode discharges show strong flows of rf power along open field lines into the divertor region. Figure 1 shows a large increase in heat flux to the outer divertor plate, when $k_{\parallel}=-8\text{m}^{-1}$ rf is coupled to an H-mode discharge (red), compared to the NBI-only case (black).

In plasmas fueled and heated by NBI, HHFW power absorption is split between electrons and fast ions in general agreement with theoretical expectations⁶. During HHFW heating of NBI plasmas the neutron production rate (S_n) increases and the fast-ion

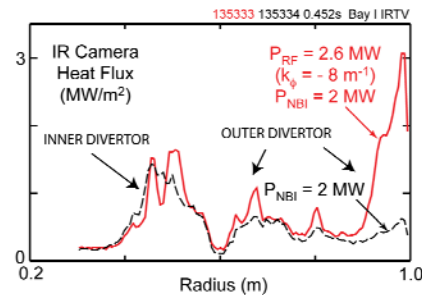


Fig.1: Divertor heat flux vs. major radius R : red, HHFW+NBI; black, NBI. (Preliminary calibration). Antenna set to $k_{\parallel}=-8\text{m}^{-1}$.

profile broadens and is enhanced⁷ (Fig.2), indicative of a significant interaction of fast waves with NBI fast ions. Data shown in Fig.2 corresponds to $k_{\parallel} = -8\text{m}^{-1}$.

Power deposition into the fast ions can be estimated by comparing the measured S_n to that predicted by the TRANSP code which includes the TORIC⁸ full-wave code, and by the CQL3D⁹ Fokker-Planck code. In Fig.3 we show the experimental neutron production rate S_n for a discharge combining HHFW and NBI auxiliary heating and for a reference discharge with NBI only. The rf target and reference discharges are consecutive $B_t(0) = 0.55\text{ T}$, $I_p = 1\text{ MA}$ deuterium plasmas with 2-MW NBI. The L-H transition occurs at 0.215s, prior to the beginning of 2-MW, $k_{\parallel} = 13\text{m}^{-1}$ (balanced), rf heating pulse at 0.25s. S_n increases during the three rf pulses. S_n predicted by TRANSP is noticeably lower than the measured value, perhaps in part because the current version of TRANSP does not self-consistently include the rf power deposition to the fast ions when evolving the fast ion distribution function.

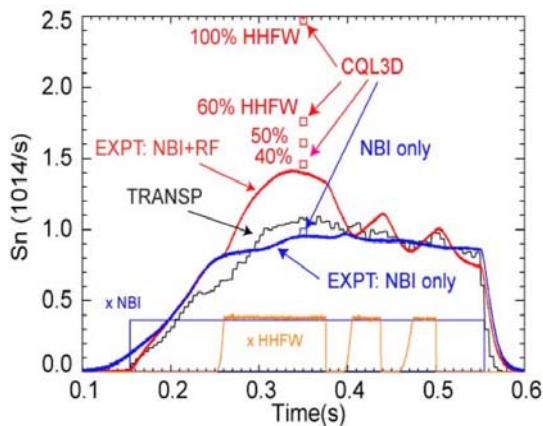


Figure3: Time evolution of measured neutron rate compared with TRANSP and CQL3D predictions. Antenna set to $k_{\parallel} = 13\text{m}^{-1}$ (balanced).

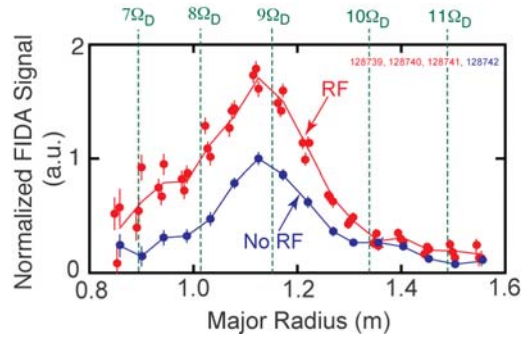


Fig.2: FIDA profiles, red, HHFW+NBI; blue, NBI. Data shown correspond to 30-65keV. Antenna set to $k_{\parallel} = -8\text{m}^{-1}$.

CQL3D was used to compute the fast-ion acceleration by the rf field assuming no fast-ion losses for decreasing fractions of the rf launched power, namely 100%, 60%, 50% and 40%. While the 40% case best matches the experimental observation, it is expected that the actual fraction of rf power coupled is higher, since some of the rf-accelerated fast ions are promptly lost on the relatively large banana orbits on the outboard side of NSTX and hence do not contribute to S_n .

*This work supported by DE-AC02-09CH11466.

¹ M. Ono, *Physics of Plasmas*, **2**, (1995) 4075

² J.R. Wilson *et al.*, *Phys. Plasmas*, **10**, No. 5, (2003) 1733

³ T. Biewer, *et al.*, *Phys. of Plasmas* **12** (2005) 056108

⁴ J.C. Hosea, *et al.*, *Phys. Plasmas* **15** (2008) 056104

⁵ M. Bell, *et al.*, *Plasma Phys. Control. Fusion* **51** (2009) 124054

⁶ B.P. LeBlanc, *et al.*, *AIP Conf. Proc.* **1187** (2010) 117

⁷ D. Liu *et al.*, *Plasma Phys. Control. Fusion* **52** (2010) 025006

⁸ M. Brambilla, *Plasma Phys. Control. Fusion* **44** (2002) 2423

⁹ USDOC/NTIS No. DE93002962 (1992); (<http://www.compxco.com/cql3d.html>)